

## The influence of cavitation on turbulent flow through a ribbed geometry

Schenker, Marieke; Delfos, R; Westerweel, J; Twerda, A; van Bokhorst, E

**Publication date**

2013

**Document Version**

Accepted author manuscript

**Published in**

Proceedings of the 8th World Conference on Experimental Heat Transfer, Fluid Dynamics and Thermodynamics, ExHFT-8, Lisbon, Portugal

**Citation (APA)**

Schenker, M., Delfos, R., Westerweel, J., Twerda, A., & van Bokhorst, E. (2013). The influence of cavitation on turbulent flow through a ribbed geometry. In *Proceedings of the 8th World Conference on Experimental Heat Transfer, Fluid Dynamics and Thermodynamics, ExHFT-8, Lisbon, Portugal*

**Important note**

To cite this publication, please use the final published version (if applicable). Please check the document version above.

**Copyright**

Other than for strictly personal use, it is not permitted to download, forward or distribute the text or part of it, without the consent of the author(s) and/or copyright holder(s), unless the work is under an open content license such as Creative Commons.

**Takedown policy**

Please contact us and provide details if you believe this document breaches copyrights. We will remove access to the work immediately and investigate your claim.

See discussions, stats, and author profiles for this publication at: <https://www.researchgate.net/publication/255991156>

# The influence of cavitation on turbulent flow through a ribbed geometry

Conference Paper · June 2013

---

CITATIONS

0

---

READS

65

1 author:



[Marieke Schenker](#)

Delft University of Technology

3 PUBLICATIONS 16 CITATIONS

SEE PROFILE

# THE INFLUENCE OF CAVITATION ON TURBULENT FLOW THROUGH A RIBBED GEOMETRY

Marieke Schenker\*, René Delfos\*, Jerry Westerweel\*, Aris Twerda\*\* and Evert van Bokhorst\*\*

\*Delft University of Technology, Mekelweg 2, 2628 CA, Delft, The Netherlands

\*\* TNO Delft, Stieltjesweg 1, 2628 CK Delft, The Netherlands.

E-mail : M.C.Schenker@TUDelft.nl

## ABSTRACT

We observe the flow through a ribbed pipe, both at ambient and lower static pressure. A smooth pipe with 4 or 5 ribs inserted at several different distances serves as the measurement section. The flow friction is dependent on the distance between the ribs, which is an effect of a change in the flow interaction of the bulk flow with the regions in between the ribs. The low pressure experiments show that the friction behavior is a function of the absolute static pressure as well. The cavitation number is the only relevant characteristic dimensionless number that changes with pressure. Plotting the pressure losses versus the cavitation number confirms the assumption that cavitation is causing the deviation from the ambient behavior, but the mechanism causing this cannot be determined from the available data. Future experiments are planned to determine the friction scaling behavior of the flow and to determine the mechanism with which cavitation interacts with the flow.

*Keywords* : Cavitation interaction, ribbed pipe, turbulence

## 1. INTRODUCTION

Flows through channels or pipes with structured geometries show many complex flow features. Scaling laws applicable to smooth surfaces or surfaces with small unstructured roughness's fail in describing structured flows and extra parameters describing the impact of the surface on the flow are required [e.g. 1]. The situation becomes even more complex when a liquid vaporizes locally within the flow. This may happen in ambient flow with strong pressure differences, but is also likely to occur in flows with near-boiling fluids. A distinction is made between boiling flow, where the vaporization is dominated by heat transfer from the surface, and cavitation, where the vapor bubbles are an effect of a local low pressure and heat transfer is less important.

This last type of flow is for example of great interest in offshore industry: When transporting Natural Gas over long distances, it is cooled down to  $-163\text{ }^{\circ}\text{C}$ , just below its boiling temperature at ambient pressure, turning it into LNG: Liquefied Natural Gas. This liquid has to be transported from one vessel to another, e.g. from ship to ship or from a ship to the shore. The design options for the transport hoses are very limited by the large discharge rates, the low temperature of the liquid and the large mechanical demands due to the motion of the sea. These factors typically result in a specific hose design, consisting of 2 thick metal helical wires with many layers of fabrics wrapped in between them, creating an inner surface with roughnesses at multiple scales. This type of hose does insulate fairly well, although never until perfection. However, the roughness introduced by the wire causes local pressure decreases, leading to cavitation.

Tests on LNG flow through such hoses showed that the pressure drop was more dependent on operating pressure than

was expected based on computations and ambient-liquid tests [2]. Local cavitation is thought to be one of the reasons causing this.

The flow in such a hose consists of two main features: It is flow through a structured geometry and it exhibits cavitation. The structure can be described as a ribbed surface, since the angle of the wire with respect to the orthogonal is negligible. The flow over ribbed surfaces is scarcely investigated [1,3,4], in contrast to the heat exchange in similar flows [e.g. 5-7], which is of great interest in optimizing heat exchangers. Boiling is often investigated in flow regimes very different from that under investigation here, such as micro-channel flows or non-flowing liquids, i.e. pool boiling. Literature covering cavitating flow is focused mostly on sheet or string cavitation at rudders or pump-blades. Cavitation in shear flows has been investigated in few papers [8,9], but no research investigating the effect of cavitation on the flow through a ribbed or corrugated pipe has been found.

The main goal of the current experiments is first to determine the scaling behavior of turbulent flow through a ribbed pipe and second to investigate how cavitation interacts with this flow.

## 2. EXPERIMENTS

Many approaches to evaluate the flow properties of rough structured flows are possible. We chose to simplify the geometry to the most basic structure, in order to grasp the most important flow features. This general approach leads to results that are widely applicable in many practical applications. The roughness of the fabric layers is not included and the helical wire is replaced by repeated ribs. In the future simple extensions to these measurements can be made by varying the shape or size of the ribs, or by adding a surface roughness to the geometry or the pipe.

For the investigation of the flow through a ribbed channel, we use tap water at room temperature. Tap water is used rather than filtered water in order to assure the availability of cavitation-nuclei in the water. For ambient pressure this method provides us with a non-cavitating flow for a large range of velocities, although for the highest velocities some cavitation appears also under ambient conditions.

For the investigation of cavitation-interaction the flow is depressurized to different static pressure levels in order to control the cavitation intensity. To determine the influence of cavitation on the pressure loss in a ribbed pipe, the cavitation intensity must be varied. Lowering the static pressure in the flow is the only manner at which cavitation-perceptibility changes independent from the other flow parameters, since all other flow parameters only depend on the pressure differences in the flow, but not on the absolute value.

## 2.1 Experimental setup

The experimental setup consists of a closed loop including a wider pressure recovery section, a centrifugal pump, a flowmeter, a run-in length of 50 diameters and a measurement section. The pressure recovery section is connected to a tank of which the pressure can be regulated by means of a vacuum-pump. A Pt-100 sensor measures the liquid temperature. We measure the pressure drop over the measurement section using a differential pressure transducer. The measurement section has 4 or 5 rectangular ribs, inserted in a smooth pipe. The distance,  $d$ , between the rib crests is variable and changes between 25 and 50 mm. A schematic image of the set-up is given in Figure 1.

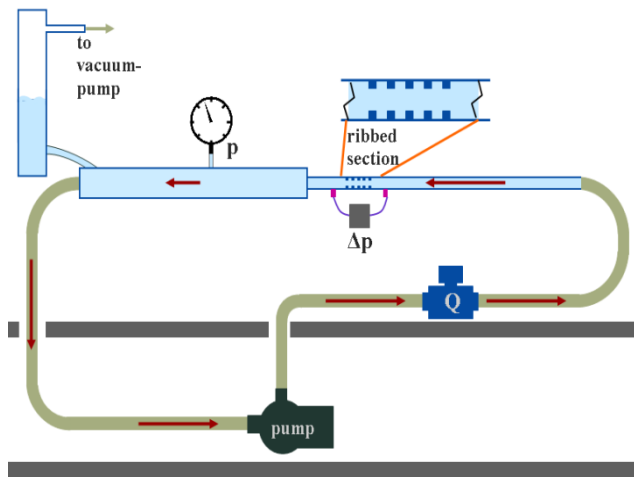


Figure 1. A schematic image of the experimental setup.

Figure 2 shows a photograph of the measurement section, with the geometric parameters explained. For the currently performed experiments the ribs have a rectangular shape, but for future experiments also rounded off ribs will be used and the ribs do not necessarily have to be equal in shape. Also, only limited by the length of the measurement section, more than 5 ribs can be used.

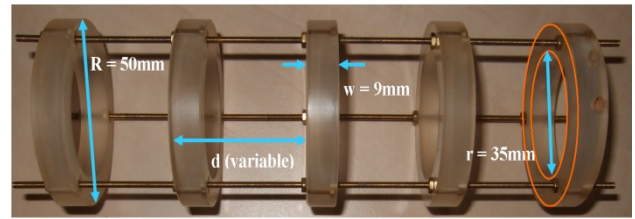


Figure 2. A photograph of the internal part of the measurement section. The relevant geometric parameters are given.

Only slightly depending on the rib configuration, the maximum reachable bulk-velocity is 6.5 m/s for all cases, leading to a maximum Reynolds number of  $\sim 3 \cdot 10^5$ . The static system pressure can reach values down to 0.2 bar absolute.

Next to the pressure loss over the measurement section also 2 hydrophones were placed in between the ribs. These sensors serve to determine the dominant frequencies in the flow, which point at the frequency of vortices shedding from the ribs. However, the obtained data has not yet been fully post-processed at the time of this writing and will not be taken into account any further.

## 2.2 Ambient experiments

The experiments at ambient pressure serve to describe the flow characteristics without the presence of cavitation. However, for the highest velocities, the pressure does reach values below the vapor pressure of water and cavitation appears. Still, non-cavitating flow has been observed for a large range of flow velocities. Currently four rib-distances, of which two with both 4 and 5 ribs have been measured. The small water column, present in the system due to the way the vacuum-chamber is connected, increases the static pressure to 1.1 bar absolute pressure rather than exactly ambient, slightly increasing the non-cavitating velocity range.

## 2.3 Low pressure experiments

For the low pressure measurements different pressure levels have been applied. The method we used to regulate the static pressure did not allow for fine tuning, the static pressure does therefore differ between the experiments. Note though that within a test, consisting of a full velocity range, the static pressure is stable.

Three rib-distances, each with 5 rings have been investigated at low pressures so far. For each geometry 8 to 10 different static pressures have been measured. The pump is capable of delivering bulk velocities up to 6.5 m/s. However, depending on the static pressure this velocity could not be reached for all cases due to leak-in of air.

As explained in the paragraph describing the experimental setup, the temperature is measured during the experiments. For the regular liquid properties the small temperature-changes present in the system are of negligible influence. However, for a cavitating flow, the temperature does have a significant effect, because the vapor pressure quite strongly changes with

temperature.

With the known and measured parameters, a dimensionless number characterizing the cavitation-susceptibility can be defined; the cavitation-number  $\sigma$  as shown in Eq. (1).

$$\sigma = \frac{p - p_0}{1/2 \rho V^2} \quad (1)$$

In Eq. (1),  $V$  and  $\rho$  represent the mean velocity through the ribs and the liquid density respectively. Note that  $V$  is unequal to the bulk velocity  $U$ .  $V$  is defined using the inner radius of the ribs,  $r$ , rather than the radius of the pipe,  $R$ . The two velocities scale with the ratio of the radii between the ribs and the pipe squared,  $(R/r)^2$ , which is  $\sim 2$  for the current geometry.

### 3. RESULTS

The ambient and low pressure experiments together provide a diverse dataset. Let us first observe the ambient flow alone. Then the influence of cavitation will be evaluated in paragraph 3.2.

#### 3.1 Ribbed flow

The mean pressure drop over 4 or 5 ribs is displayed in non-dimensional form using the parameter  $K$ , which is the ratio between the pressure drop and the velocity squared:

$$K = \frac{\Delta p}{1/2 \rho U^2} \quad (2)$$

For a fully turbulent flow this  $K$  is expected to be a constant, of which the value depends on the geometry only. In Eq. (2), the bulk-velocity  $U$  is used, instead of  $V$  as was the case in the definition for the cavitation number. This enables us to compare the results of different rib inner diameters, although for the current measurements only 1 rib size has been used.  $K$  has been plotted versus  $1/2\rho U^2$  in Figure 3. In the plot, the three continuous lines represent three different rib-distances with 5 ribs, the two dashed lines show the corresponding geometries with only 4 ribs.

For a large range of velocities within the plot the  $K$  value is indeed constant. For the lower velocities, the value deviates because the flow is not yet fully turbulent. For the highest velocities cavitation appears and the flow does no longer behave like a single phase flow, leading to a deviation from the horizontal. The difference between the cases with 4 and 5 rings indicate the influence of a single rib. This is of importance, because we are eventually interested in an “infinite” ribbed section, and the extra effect of the first ring should thus be excluded from the results.

As can be seen for the ribs at 50 mm distance, the difference in pressure drop between the experiments with 4 and 5 ribs is much larger than at 25 mm distance. When assuming this pressure drop for every rib, the difference for the 50 mm distance is even larger than what is physically possible. This is probably

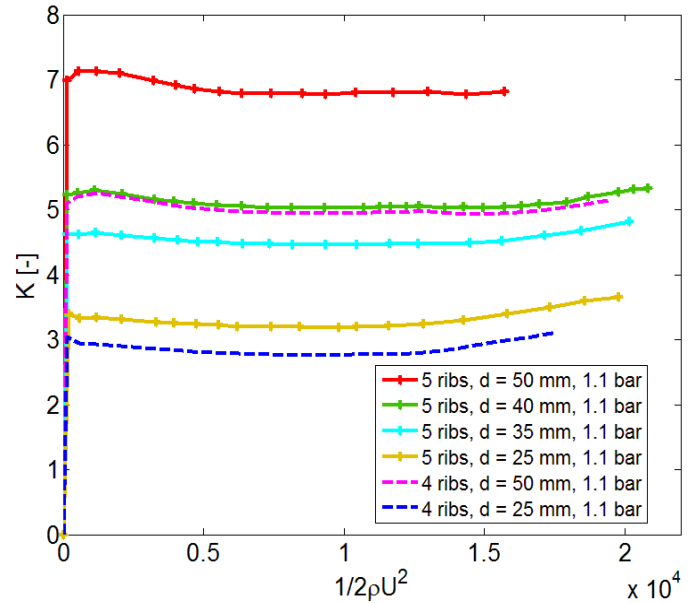


Figure 3.  $K$  versus  $1/2\rho U^2$  for all 6 geometries at 1.1 bar static pressure.

an effect of the first rib, which is still influencing the flow at the location of the last rib. However, the large difference between the two geometries still indicates a different regime in the flow through the ribbed section.

#### 3.2 Influence of low pressure

Combining the experiments performed at ambient pressure and those at lower pressures provides us with information regarding the influence of cavitation on the flow losses.

Figure 4 shows  $K$  versus  $1/2\rho U^2$  for only 1 geometry (i.e. rib distance 35 mm), but for a whole range of absolute pressures.

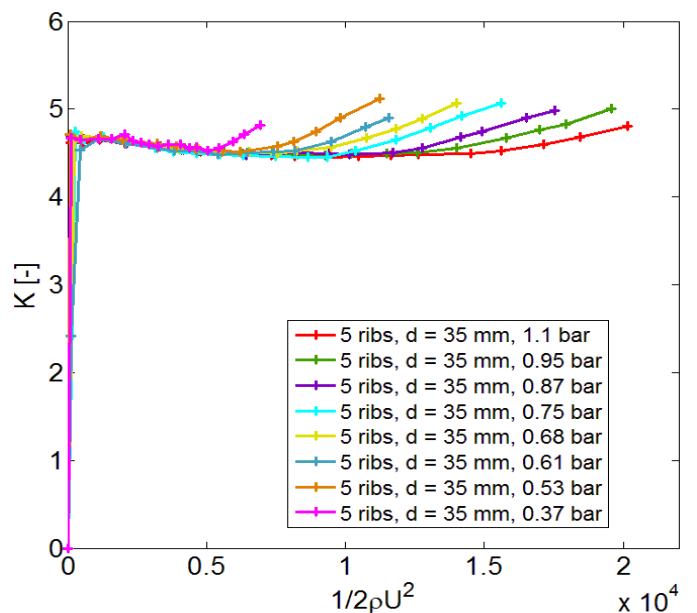


Figure 4.  $K$  versus  $1/2\rho U^2$  with 5 ribs and  $d = 35$  mm for a range of static pressures.

The influence of the absolute pressure is clearly visible. A lower pressure results in an earlier deviation from the constant value. The same behavior can be observed for all rib-distances, but for clarity only one has been plotted in Figure 4.

The Reynolds number has not changed with the static pressure, but the cavitation number is different for different pressures. It is therefore logical to plot  $K$  versus  $\sigma$  to see whether all differences can be accounted for by the appearance of cavitation. This is shown in Figure 5 for all geometries with 5 ribs. For 4 ribs the same effect occurs, but plotting those makes the graph unclear because curves cross each other.

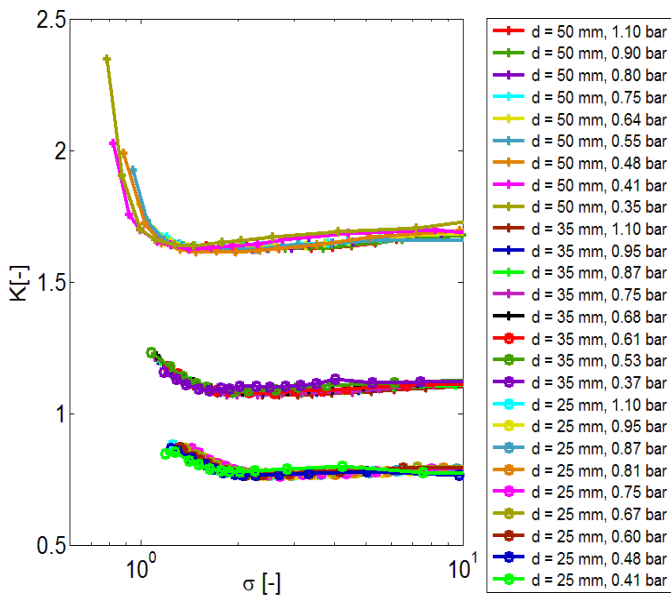


Figure 5.  $K$  versus  $\sigma$  for 3 rib-distances  $d$ .

The curves corresponding to a single geometry do overlap very well. Note that the cavitation number is plotted on a logarithmic scale and the graph is cut-off for cavitation number higher than 10. This emphasizes the region of interest, with the cavitation numbers close to and below the cavitation threshold. Since the cavitation number is only a relevant parameter when cavitation occurs the graph has no meaning for the non-cavitating flow corresponding to high cavitation numbers.

Theoretically the threshold for cavitation to occur lies at  $\sigma=1$ , but in practice this threshold is slightly different. The main cause for this difference is that the location where the lowest pressure occurs never on the same location is as where the pressure is measured or can be predicted based on the measurements. Because of this the threshold cannot be defined exactly.

As can be seen in Figure 5, the cavitation number at which  $K$  starts increasing depends on the geometry. For the geometries with ribs closer to each other  $K$  starts increasing at higher cavitation number.

Besides this shift in onset, another difference is observed in the behavior of the different rib-distances. For the smallest rib distance,  $K$  is almost constant for the larger cavitation-numbers, and then starts increasing. For the larger rib-distances a more

complex behavior seems to occur.  $K$  first decreases slightly before increasing again.

Some curves do not extend to the lowest cavitation numbers. This is an experimental issue. The lowest cavitation numbers do correspond to the lowest static pressures. Since the whole flow loop experiences this low pressure, it is crucial that the whole loop is completely air-tight. However, the system does experience some air leak-in at the lowest pressures. When air was detected in the system the experiment was terminated, because cavitation is strongly suppressed when gas is present in the flow.

Some visual observations were made during the measurements. Other than expected, in most cases, the first visible appearance of cavitation-bubbles occurred on the first rib. Only for the case with 5cm distance the cavitation appeared first at the rib most downstream.

Cavitation is also detected by its sound. The first appearance can be categorized as "sputter": soft, distinct short sound bursts, irregular in time. A second stage is a more regular sputtering, followed by state 3: continuous sound. The 4th and 5th stage are similar, but louder. Eventually the sound becomes a "zooming sound", probably caused by vibration of the ribs in the pipe rather than the cavitation itself.

The different observations of both sound and visible cavitation are logged and will be used to clarify the relation between cavitation and pressure behavior in the flow.

#### 4. CONCLUSIONS

The results at ambient pressure indicate indeed a regime change between the different rib distances. This regime change is caused by the way the main flow interacts with the regions in between the ribs. The effect of a single rib is indicated by comparing a ribbed section with 4 and 5 ribs. However, the results for the largest rib distance indicate that a second effect plays a role, since the resistance obtained for a single rib exceeds 1/4<sup>th</sup> of the total. Most likely this is an effect of the first rib, extending all over the ribbed section. The observation that for most geometries cavitation initiates at the first rib is a strong indication for a distinct flow at the first rib, resulting in a strong flow-contraction with respect to the flow through the other ribs.

The influence of cavitation is investigated by decreasing the static pressure in the system, and thereby increasing the cavitation intensity. Significant changes in the pressure loss, expressed in its dimensionless form  $K$ , are shown for all rib distances. When plotting versus the cavitation number rather than the velocity squared the curves corresponding to a single geometry collapse on to each other, regardless of the static pressure. This is a clear indication that it is indeed cavitation that causes the pressure-loss to deviate from the ambient flow behavior. However, the mechanism that causes the increase in friction cannot be determined from the performed experiments alone. One factor certainly leading to an increase in pressure loss is the increased volume due to the local vaporization. Another proposed mechanism is a modification of the shear layer shed by the ribs [8].

#### 4.1 Future work

To be able to determine the scaling behavior as a function of the rib-distance many more different geometries must be measured. Also a geometry with a rib distance smaller than the rib height must be measured, while from literature we know that this geometry results in a complete different flow regime when used in channel flow.

While the first rib is of great influence to the flow, due to the sudden area blockage it causes, it is of little interest to the actual problem, and we would therefore like to minimize its effect on the flow. In future experiments we will modify the shape of the first rib in order to decrease the flow contraction at the edge and the influence downstream inside the ribbed section. When more flow-data is available, the logged information concerning the visual and audible observations of cavitation can be helpful to determine the interaction mechanism between cavitation and flow.

Also the hydrophone measurements that have been made must be processed. These measurements serve to provide us with the typical flow frequencies, including the shedding frequency, at with vortices shed from the ribs. When, as indicated by [9], the cavitation interacts with the vortices in the shear layer, this should lead to a change in shedding frequency.

For further examination of the influence of cavitation on a ribbed flow it is of importance to determine the volumetric fraction of the vapor. This fraction provides a measure of the expected pressure loss increase purely based on the extra volume. The next step in the experimental process will therefore be visualizing the vapor bubbles by high speed imaging. This will provide us with both the spatial bubble distribution within the geometry and the size-distribution of the bubbles. These distributions together will be used to derive the volume fraction of the vapor in the liquid.

#### REFERENCES

1. J. Jimenéz, Turbulent flows over rough walls, *Annu. Rev. Fluid. Mech.*, vol 36, pp. 173-196, 2004.
2. B. van den Beemt, E. van Bokhorst, G. van der Weijde, N. Mallon and S. Verweij, Qualification of LNG STS Transfer flexibles according to guideline EN1474-2, *Proc. Offshore Technology Conference*, Houston, Texas, 4-7 May 2009.
3. J. Cui, V.C. Patel and C. Lin, Large-eddy simulation of turbulent flow in a channel rib roughness, *Int. J. Heat Mass Transfer*, vol 24, pp. 372-388, 2003.
4. S. Vijapurapu and J. Cui, Simulation of turbulent flow in a ribbed pipe using Large Eddy Simulation, *Numer. Heat Transfer, Part A*, vol.51, pp. 1137-1156, 2007.
5. T. Liou, J. Hwang and S. Chen, Simulation and measurement of enhanced turbulent heat transfer in a channel with periodic ribs on one principal wall, *Int. J. Heat Mass Transfer*, vol 36, pp. 507-517, 1993.
6. H. Sato, Characteristics of turbulent flow and heat transfer in a rectangular channel with repeated rib roughness, *Experimental Heat Transfer*, vol 5, pp. 1-16, 1992.
7. R.L. Webb, Heat transfer and friction in tubes with repeated-rib roughness, *Int. J. Heat Mass transfer*, vol 14, pp. 601-617, 1971
8. C.O.Lyer and S.L.Ceccio, The influence of developed cavitation on the flow of a turbulent shear layer, *Physics of Fluids*, vol 14, number 10, pp. 3414-3431, Oct. 2002.
9. T. Ohta, H. Sakai, K. Okabayashi and T. Kajishima, Investigation of interaction between vortices and cavitation in a turbulent shear layer, *J. Fluid Science Technology*, vol 5, number 6, pp. 1021-1035, 2011.